The Resurgence of the Linear Optics Interferometer — Recent Advances & Applications

Si-Hui Tan[1,2,*] and Peter P. Rohde[3,†]

[1]*Singapore University of Technology and Design, Singapore University of Technology and Design, 8 Somapah Rd, Singapore 487372*
[2]*Centre for Quantum Technologies, National University of Singapore, Block S15, 3 Science Drive 2, Singapore 117543, Singapore*
[3]*Centre for Quantum Software & Information (CQSI), Faculty of Engineering & Information Technology, University of Technology Sydney, NSW 2007, Australia*

Contents

---

*[*]sihui_tan@sutd.edu.sg
[†]dr.rohde@gmail.com; URL: http://www.peterrohde.org

I. INTRODUCTION

To do

Technical advancements have been made on many fronts. It is possible now to put single-photon sources and linear-optical networks on a silica chip. The advantage of using such integrated photonics over bulk optics is that it is more stable against phase fluctuations, and miniaturized. This increases the scalability of optical implementations of quantum information protocols.

II. MATHEMATICAL BACKGROUND

A idealized single photon in a quantum interferometer is described by its creation operator $\hat{a}_j^\dagger$, where j is the label of the mode the photon is in within the interferometer. The creation and annihilation operators satisfy the bosonic comutation relationship $[\hat{a}_j, \hat{a}_k^\dagger] = \delta_{j,k}$. A similar commutation relationship can be written when additional degrees of freedom, such as polarization, orbital angular momentum, and time-bins (Tillmann et al., 2015; Bozinovic et al., 2013; Nicolas et al., 2014; Humphreys et al., 2013; Donohue et al., 2013), are present. When multiple photons are present, they experience quantum interference when all quantum labels are the same.

The action of a $2d$-port linear optical interferometer (with an equal number of input and output ports) is expressed as an application of unitary operations on the creation operators,

$$b_i^\dagger = \sum_{j=1}^d U_{ij} a_j^\dagger \,, \tag{1}$$

where $a_j^\dagger$ and $b_i^\dagger$ are the creation operators of a single input and output photon in the j-th and i-th modes respectively, and $U \in SU(d)$. All such transformations can be expressed as sequences of beamsplitters and phase-shifters (Reck et al., 1994). In the case when photons have additional labels, for instance, if they have internal labels on top of spatial labels, it is also possible to derive an analogous decomposition, known as a cosine-sine

decomposition (Dhand and Goyal, 2015), that realizes the unitary transformation on the photons as a sequence of beamsplitters and internal transformations. Toolkits using group theory are being developed to deal with partial distinguishabilities among interfering photons (Tan et al., 2013; de Guise et al., 2014, 2016). Others use quantum-to-classical transitions to explain multiparticle interference (Ra et al., 2013). Experimental implementation [Walmsley, Jennewein]

III. OPTICAL ENCODING OF QUANTUM INFORMATION ON SINGLE-PHOTONS

Using quantum states of light, there are a multitude of approaches to encoding quantum information. Beginning with a logical qubit,

$$|\psi\rangle_L = \alpha|0\rangle_L + \beta|1\rangle_L, \qquad (2)$$

we now discuss the most prominent such encodings, which have been widely employed. We will specifically focus on single-photon encodings, as opposed to, for example, continuous variable encodings.

These encodings are all isomorphic to one another, but nonetheless, because they are represented using entirely different physical systems, they each exhibit their own unique advantages and disadvantages, and methods by which to implement operations upon them.

1. Polarisation

In polarisation encoding, the polarisation of a single photon in a single spatial mode encodes a logical qubit. Specifically, we represent the logical qubit as,

$$|\psi\rangle_L = \alpha|H\rangle + \beta|V\rangle, \qquad (3)$$

where H (V) denotes a horizontally (vertically) polarised single photon.

Polarisation encoding has the elegance that the most common optical error mechanisms, such as loss or path-length mismatch, affect the two logical basis states equally. Furthermore, single-qubit operations may be directly implemented using wave-plates, which implement a rotation in polarisation space. Relevant to the preparation of large entangled states, such as cluster states, polarising beamsplitters can be employed to perform non-deterministic Bell state projections.

When physically constructing protocols based on polarisation-encoding, for obvious reasons it is extremely important that optical components be polarisation-preserving. Not doing so would obviously corrupt the logical state. Some waveguide technologies, for example, exhibit different refractive indices for the two polarisations.

2. Dual-rail

In dual-rail encoding, a single photon encodes a logical qubit as a superposition across two spatial modes,

$$|\psi\rangle_L = \alpha|1,0\rangle + \beta|0,1\rangle, \qquad (4)$$

where $|i,j\rangle$ is a two-mode state with i (j) photons in the first (second) spatial mode. Using this encoding, phase-shifters and beamsplitters between the two spatial modes implement arbitrary single-qubit operations. Converting between polarisation- and dual-rail-encoding is trivial using polarising beamsplitters, which separate horizontal and vertical components into distinct spatial modes, or vice-versa.

Unfortunately, because the two basis states evolve via independent paths, our dual-rail qubits are susceptible to path-length-mismatch, a problem that does not affect polarisation encoding. Nonetheless, there are certain advantages to using two paths as opposed to one as is the case in single-rail encoding where the presence or absence of a photon denotes the logical bit. The loss of a photon in a dual-rail qubit is easily noted by its absence, whereas in a single-rail encoding, it would have been confused for one of the states. Moreover, a no-go result precludes universal quantum computation using just linear optics without the use of measurements in a single-rail encoding (Wu et al., 2013), thus making dual-rail encoding a more attractive alternative.

3. Time-bins

Time-bin qubits encode quantum information into the time-of-arrival of single photons, which have fixed polarisation and reside in a single spatial mode. Effectively, we discretise the direction of propagation of photons into discrete bins, which are treated as orthogonal basis states. Specifically, we are employing the encoding,

$$|\psi\rangle_L = \alpha|1\rangle_t|0\rangle_{t+\tau} + \beta|0\rangle_t|1\rangle_{t+\tau}, \qquad (5)$$

where $|0\rangle_t$ ($|1\rangle_t$) denotes the vacuum (single-photon) state with arrival time t. Here τ is the time-bin separation, which must be sufficiently large that the temporal envelopes of neighbouring photons do not overlap, thereby ensuring orthogonality of the logical basis states.

This encoding is particularly resource-savvy, since a single spatial mode (e.g length of optical fibre) can encapsulate many time-bin qubits as a 'time-bin-train'. The amount of quantum information that can be encoded into the train is limited only by its physical length.

Unlike polarisation or dual-rail encoding, time-bin encoding does not lend itself to 'native' single-qubit operations. Rather, fast switching can be used to spatially separate neighbouring time-bins, implement a beamsplitter operation between them, before converting back to time-bin encoding.

Time-bin encoding was first conceived via a single-photon passing through a Mach-Zedner interferometer

with its two paths having different lengths (Brendel et al., 1999). If the photon passes through the shorter (longer) path, it will arrive at the output port in an 'early' ('later') time-bin labelled $|e\rangle$ ($|\ell\rangle$). Thus, the photon will exit the interferometer in a state that is a superposition of these two states. Owing to difficulties in implementing qubit operations in this basis, it was at the time mostly used for demonstrating quantum communication over long distances (Thew et al., 2002; Marcikic et al., 2004). With the advent of faster optical components, and single-photon detectors, it has become feasible to perform any single qubit operation, and a post-selected CPHASE gate on time-bin qubits (Humphreys et al., 2013). These gates form an universal set for quantum computing. At the same time, an ultrafast measurement technique for recovering time-bin qubits was also demonstrated (Donohue et al., 2013).

In Humphrey et al. (Humphreys et al., 2013), the time-bin qubits have a polarization register which is used to toggle between the mode in which qubits are stored and transmitted, i.e. the 'register' mode, and the mode in which qubits are manipulated, i.e. the 'processing' mode using a polarization rotation. Other operations needed are a displacement operation, that moves a time-bin qubit in the processing polarization in time relative to other qubits, a partial polarization rotation between the register and processing polarizations to couple them, and a photon number measurement in a bin. The polarization rotation and polarization coupling operations were implemented using a fast integrated optical switch based on polarization-sensitive cross-phase modulation with a switching time of less than 10ps. The displacement was implemented using a calcite crystal of a size that is of a path-length difference equal to an integer multiple of the time-bin separation. Using these operations and post-selection using a single-photon detectors, the authors were able to perform a heralded CPHASE gate (Knill et al., 2001).

In Donohue et al. (Donohue et al., 2013), time-bins were converted into frequency bins using a nonlinear optical process known as sum-frequency generation (SFG) by pumping them on a crystal with a laser beam. The waveforms of the input photons and the pump beam are chirped in opposite directions in frequency, so that the output is a set of two peaks separated in frequency by an amount proportional to the time separation of the time bins. The output can then be measured with detectors that are slow compared to this separation. This is unlike conventional time-bin measurements which involve sending a time-bin state through an unbalanced Mach-Zedner interferometer matched to the time-bin separation to produce three output pulses that are separated by the time delay, and then having to resolve the middle pulse in time.

Apart from these promising advances in implementing time-bin qubit gates and ultrafast time-bin measurements, scalable networks using time-bin encoding are also possible using a loop-based architecture (Motes et al.,

2014). This is discussed in more detail in Section VI.B.3.

IV. EFFICIENT CIRCUIT DECOMPOSITIONS OF LINEAR OPTICS NETWORKS

The task of implementing an arbitrary quantum computation on linear optics comes down to implementing an arbitrary $n \times n$ unitary matrix. If a non-unitary transformation is desired, it can be embedded within a unitary matrix with larger dimensions. An algorithm for expressing an arbitrary unitary matrix *exactly* in terms of a sequence of beamsplitters and phase-shifters was described by Reck *et al.* (Reck et al., 1994). This decomposition requires $\mathcal{O}(n^2)$ linear optical elements, and the algorithm for finding the decomposition has polynomial runtime. Thus, such decompositions can always be determined and implemented efficiently. The layout for the original Reck *et al.* decomposition is shown in Fig. 1. However, since then a multitude of alternate decompositions have been found. A notable downside of the original decomposition is that different photons experience different circuit depth, i.e pass through different numbers of optical elements, resulting in asymmetry in losses and the accumulation of errors.
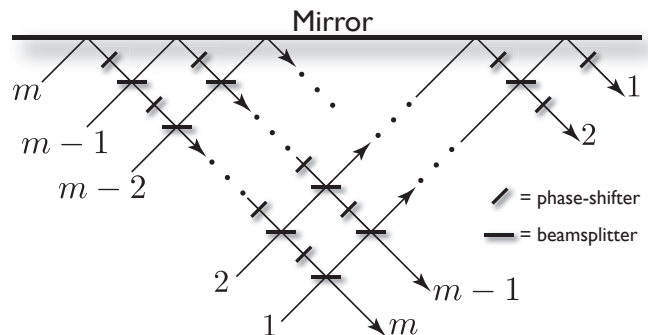

FIG. 1 Efficient decomposition of arbitrary linear optics networks into a sequence of beamsplitters and phase-shifters.

Alternatively, Mach-Zedner interferometers can also be employed as building blocks instead of beamsplitters and phase-shifters (Reck et al., 1994; Englert et al., 2001). Later, it has been shown that any nontrivial beamsplitter, that does more than permuting modes or adding phases to them, is universal for linear optics (Bouland and Aaronson, 2014). However, they do not provide an explicit construction for arbitrary unitaries.

If the linear optical transformations can be realized on various degrees of freedom of light, then it is possible to realize a $n \times n$ arbitrary unitary transformation, where $n = n_s n_p$ for n_s spatial modes, and n_p internal modes, by a sequence of $\mathcal{O}(n_s^2 n_p)$ beamsplitters and $\mathcal{O}(n_s^2)$ internal transformations (Dhand and Goyal, 2015). Their approach reduces the required number of beamsplitters but increases the total number of optical elements needed by a factor of 2.

V. RECONSTRUCTING THE LINEAR OPTICAL NETWORK

In many practical situations, the structure of a linear optical device in terms of its constituent beamsplitters and phase-shifters is known once it is built. However, owing to manufacturing imperfections, a precise characterization of these devices is still needed post-production. One approach for achieving this is via quantum process tomography (Mitchell et al., 2003; O'Brien et al., 2004; Lobino et al., 2008; Rahimi-Keshari et al., 2011). However, quantum process tomography is an expensive approach in terms of the number of measurements required to characterize the network, with exponential overhead, becoming impractical for large optical networks which can contain hundreds of modes using present-day technology (Harris et al., 2016). However, alternative characterization protocols have been developed using quantum interference of various quantum light sources (Laing and O'Brien, 2012; Rahimi-Keshari et al., 2013) in the linear optical device.

Generally, the unitary matrices of $d \times d$ linear optical devices are complex $U_{ij} = r_{ij}e^{i\theta_{ij}}$, where $0 \leq r_{ij} \leq 1$, and $0 \leq \theta_{ij} \leq 2\pi$. The scheme in (Laing and O'Brien, 2012) relies on injecting one- and two-photon states into the network with correlated photon detection. First, they note some equivalencies: two unitaries U and U' are equivalent if there exist two diagonal unitary matrices D_1^U and D_2^U such that $U' = D_1^U U D_2^U$, because these diagonal matrices are regarded as unknown and trivial phases on the input and output ports of the network, to which the one- and two-photon data are insensitive to. This reduces the first row and column elements to real numbers, i.e. $\theta_{1j} = \theta_{i1} = 0$. Second, the photo-statistics remain invariant under complex conjugation by U. Thus, the imaginary part of $M_{2,2}$ must be non-negative. Then, assuming the first two rows and columns are non-vanishing, and there is no total loss in the interferometer, the matrix to be recovered is

$$U = \begin{pmatrix} r_{11} & r_{12} & \dots & r_{1m} \\ r_{21} & r_{22}e^{i\theta_{22}} & \dots & r_{2m}e^{i\theta_{2m}} \\ \vdots & \vdots & \ddots & \vdots \\ r_{m1} & r_{m2}e^{i\theta_{m2}} & \dots & r_{mm}e^{i\theta_{mm}} \end{pmatrix} . \quad (6)$$

They showed it is possible to write the parameters r_{ij}, and θ_{ij} for $i,j \geq 2$ in terms of the $2m-1$ real parameters of the first column and row, and the visibility of two-photon inputs. The remaining $2m-1$ real parameters can be found via one-photon transmissions. An increased accuracy in the characterization is possible by estimating and correcting systematic errors that arise due to mode mismatch (Dhand et al., 2016). Others have used numerical methods to find the closest parameters that yield the observed visibilities (Spagnolo et al., 2016; Tillmann et al., 2016).

Another characterization method was presented that is similar to (Laing and O'Brien, 2012) with the important exception that coherent states are to be used instead of Fock states (Rahimi-Keshari et al., 2013; Heilmann et al., 2015). Such states are produced by a standard laser source, thus reducing experimental resources. The r_{jk} terms are found by the square root of the ratios of output intensities at the kth port to the input intensity at the jth port. The remaining phases θ_{ij} are found by the interference pattern given by a two-mode coherent state $|\alpha_1\rangle|\alpha_2\rangle$ created by splitting a single coherent state on a 50-50 beamsplitter, and then imparting a relative phase, ϕ, between them. The states $|\alpha_1\rangle$ and $|\alpha_2\rangle$ are input into port 1, and j respectively. The output intensity at the jth port is then

$$I_k = I(r_{1k}^2 + r_{jk}^2 + 2r_{1k}r_{kj}\cos(\phi + \theta_{jk})) , \quad (7)$$

where $\theta_{jk} = 0$ for $k = 1$. By scanning the phase shift ϕ and locating the maximum value of I_k for $j = 2,\dots,m$, all unknown phases can be found via $\theta_{jk} = 2\pi - \phi$. An elegant extension of the scheme of Rahimi-Keshari et al. removes the need for precise control of the phase-shift ϕ (Heilmann et al., 2015) by suggesting instead to plot the output intensity I_k with respect to the input intensity I. In time, the natural drift in the laser source will cause this plot to trace out an ellipse, known as a Lissajous figure, whose orientation and direction of evolution will give the phase θ_{jk} and its sign respectively.

VI. EXPERIMENTAL IMPLEMENTATION

Significant progress has been made in the experimental realisation of linear optics protocols, and have become standard and widespread. We now discuss some of these advances.

A. State preparation

The photonic states that are most commonly employed in linear optics protocols can be divided into Fock states (e.g single-photon), and entangled states, such as EPR, GHZ and cluster states. We will consider advances in each of these.

1. Single-photons

Sources of single photons for applications in quantum information processing can be separated into two main categories: those produced by spontaneous parametric down-conversion (SPDC), and those by solid-state emitters in a cavity. Both categories have seen major development recently in photon-number, with high fidelities. To-date, SPDC has been able to produce up to ten entangled photons (Wang et al., 2016a; Chen et al., 2017), and five-photon quantum interference has been reported using a quantum dot emitter in a microcavity (Wang et al., 2016b).

In SPDC, a nonlinear crystal with a large $\chi^{(2)}$ nonlinearity is pumped with a strong coherent state (i.e laser source) and with a small probability, the pump beam is absorbed by the crystal to produce two beams of lower energy known as the signal and idler. Owing to conservation of energy and momentum, the two beams have spatio-temporal correlations that can be engineered to produce twin-beam states with perfect photon number correlation, of the form

$$|\psi\rangle_{\mathrm{SPDC}} = \sqrt{1-\chi^2} \sum_{n=0}^{\infty} \chi^n |n,n\rangle, \qquad (8)$$

where χ is the squeezing parameter. If a single photon were to be detected in one of the modes, it is certain that the other mode would similarly contain a single photon.

Some commonly used nonlinear crystals for SPDC are beta barium borate (BBO), periodically poled lithium niobate (PPLN), and periodically poled potassium titanyl phosphate (PPKTP). Recently, techniques using bismuth triborate (BiBO) have improved to the extent of becoming one of the record-holders in single-photon production (Wang et al., 2016a).

Solid-state single photon sources come from semiconducting nanostructures and nitrogen valencies (NV) centers in diamond. Both types are versatile and efficient sources of single photons, however, the photons they produce have suffered from the lack of indistinguishability that is necessary for typical quantum information processing applications. Recent developments in the former have been very promising. Notably, much progress has been made using resonant excitation of quantum dots. Here, laser pulses are used to excite their electronic resonance and trigger the emission of single photons (Muller et al., 2007; Nick Vamivakas et al., 2009; Flagg et al., 2009; Ates et al., 2009; Englund et al., 2010; He et al., 2013a; Jayakumar et al., 2013; Wei et al., 2014; Muller et al., 2014; Unsleber et al., 2015; He et al., 2013b; Sweeney et al., 2014). An architecture that embeds the quantum dot in a micropillar cavity with the same resonant frequency as the dot exploits the Purcell effect to achieve higher single-photon production efficiency(Ding et al., 2016; Wang et al., 2016c). Such resonant excitation of quantum dots overcomes the homogenous broadening of the excited state that causes degradation of photon purity and improving indistinguishability. Using a time-bin loop-based architecture (Motes et al., 2014) on a stream of single photons produced by such a quantum dot, the same group was able to demonstrate quantum interference between five indistinguishable photons (Wang et al., 2016a).

2. Einstein-Podolsky-Rosen (EPR) pairs

An EPR pair, or Bell pair, is one of the four states,

$$|0\rangle_A |0\rangle_B \pm |1\rangle_A |1\rangle_B,$$
$$|1\rangle_A |0\rangle_B \pm |0\rangle_A |1\rangle_B, \qquad (9)$$

which are all maximally entangled and locally equivalent to one another. These are the simplest examples of entangled states, and their preparation via SPDC has been the mainstay of entangled state preparation for quantum optical processing (Kim et al., 2001, 2003; Brida et al., 2007; Dayan et al., 2007). In some applications, it may be desired to have the EPR pairs conditionally prepared, *i.e.* successfully prepared only under certain measurement outcomes of auxiliary modes. Several theoretical approaches have been proposed for this purpose (Pittman et al., 2003; Śliwa and Banaszek, 2003; Walther et al., 2007), and demonstrated (Wagenknecht et al., 2010; Barz et al., 2010). They are often used as a building block for preparing other multipartite entangled states.

3. Greenberger-Horne-Zeilinger (GHZ) states

GHZ states form a class of entangled quantum states on multiple subsystems with at least three parties (Greenberger et al., 1989). For qubit encodings with n subsystems, a GHZ state is of the form

$$|\Psi_n^{(\mathrm{GHZ})}\rangle = \frac{|0\rangle^{\otimes n} + |1\rangle^{\otimes n}}{\sqrt{2}}. \qquad (10)$$

These states are also non-local, and have been used extensively in experimental test for non-locality (Pan et al., 2000; Zhang et al., 2015). This has been a subject matter covered in detail by another review (Pan et al., 2012).

4. Cluster states

Cluster states form another class of multiparty entangled states, and were conceived in the context of arrays of qubits with an Ising-type interaction (Briegel and Raussendorf, 2001).

These states can be represented as a graph, in which vertices are qubits initialized into the superposition state $|+\rangle = \frac{1}{\sqrt{2}}(|0\rangle + |1\rangle)$, with CPHASE operation applied between edges, as shown in Fig. 2. For this reason, such states are also referred to as graph states. The CPHASE operations generate entanglement between the qubits, and because they commute, are independent of ordering. Cluster states are a resource state for a model of quantum computation known as measurement-based quantum computation (MBQC). Here, having such a state as a resource enables universal quantum computation using only single-qubit measurements (Raussendorf et al., 2003). Therefore, the preparation of such states is highly valuable, generating much interest in their efficient preparation.

Unfortunately, implementing CPHASE gates using linear optics is complicated and highly non-deterministic. A major improvement upon this is to use fusion gates - rotated polarising beamsplitters, which implement projections onto the Bell basis. These operations fuse smaller cluster states, represented using polarisation encoding,
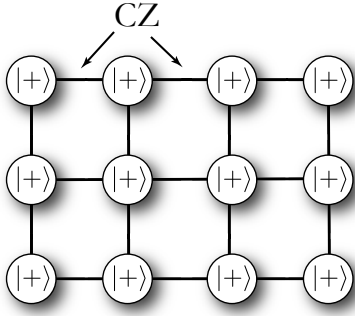
FIG. 2 The representation of cluster states as a graph. Vertices represent qubits initialised into the $|+\rangle$ state, while edges represent the application on CPHASE gates, the ordering of which is irrelevant.

into larger ones, consuming one (type-I fusion) or two (type-II fusion) photons in the process. These operations are shown in Fig. 3. Although these operations are non-deterministic with a success probability of 1/2, they require only a single beamsplitter, already a major improvement over directly implementing CPHASE gates. Furthermore, unlike CPHASE gates, fusion operations require only high Hong-Ou-Mandel visibility, rather than the Mach-Zehnder stability required within existing CPHASE gate implementations, a major experimental simplification.

Although these gates are non-deterministic and consume qubits, strategies have been described for efficiently preparing arbitrarily large cluster states of arbitrary topology, and using far fewer optical elements than by directly employing CPHASE gates.
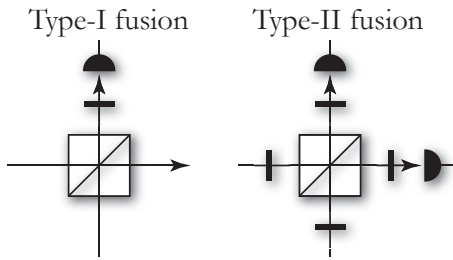

FIG. 3 Fusion gates for joining smaller cluster states into larger ones. Both require only a single polarising beamsplitter, and waveplates. The type-I and -II fusion gates consume 1 or 2 qubits (photons) respectively, creating an edge between the remaining graphs. The type-I gate consumes one fewer photon, but requires number-resolved detection on the detected mode. The type-II gate requires only on/off photodetection, but consumes an additional photon. Thus, the type-I gate can be employed to fuse two Bell pairs into a 3-qubit cluster state, whereas the type-II gate will only grow clusters when beginning with at least 3 qubits per cluster.

B. Linear optics networks

Numerous experimental implementations of various linear optics protocols have been demonstrated, using a variety of architectures. The main contenders considered to date are: bulk-optics; waveguides; and time-bin encoding.

1. Bulk-optics

The early implementations of linear optics protocols relied on bulk-optics implementations, in which a circuit is decomposed into a discrete arrangement of optical components, specifically beamsplitters and phaseshifters. This corresponds to a direct implementation of the Reck *et al.* decomposition shown in Fig. 1, or subsequent alternate decompositions.

Although this approach is effective and conceptually straightforward, it is highly impractical for large interferometers. For example, the implementation of a 100-mode interferometer requires on the order of 10,000 discrete optical elements, which must all be simultaneously aligned with interferometric stability, a highly experimentally challenging problem, not to mention incredibly physically large.

2. Waveguides

Alternately, integrated waveguide devices can be employed to implement identical decompositions by etching the modes into paths in an optical chip, where evanescent coupling between closely neighbouring modes implements beamsplitter operations. Such devices are extremely compact, allowing the miniaturisation of large numbers of optical elements. Importantly, such devices are extremely optically stable, mitigating the need for any kind of dynamic stabilisation

3. Time-bins

Using time-bin encoding of optical qubits, the obvious question is how to perform operations upon them. In (Motes et al., 2014), a dual-loop architecture was presented for implementing arbitrary passive linear-optics on photonic pulse-trains, shown in Fig. 4.

The architecture is frugal in its use of optical components, requiring only three dynamic beamsplitters, and several lengths of fibre. The beauty of this architecture is that the experimental requirements do not increase with the number of optical modes. The only parameter that scales with the number of optical modes is the outer loop, which must be at least long enough to house the entire time-bin-encoded pulse-train. Note, however, that the central beamsplitter must be controllable at sub-τ time-scales, so as to enable each temporal mode to be addressed individually, which is technically challenging.
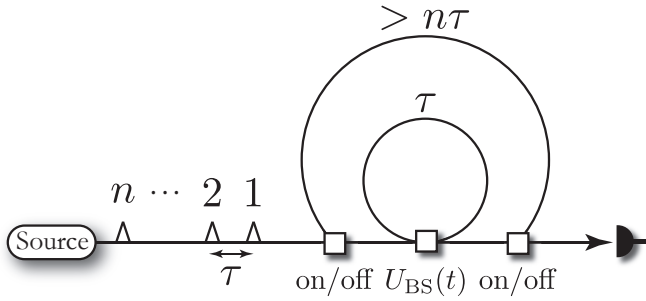
FIG. 4 A fibre-loop architecture for implementing arbitrary linear optics operations upon a time-bin-encoded pulse-train. The source prepares the temporally encoded pulse-train, with time-bin separation τ. The pulse-train then enters a dual-loop configuration. The inner loop has length exactly τ, while the outer one has length $> n\tau$ (n is the number of optical modes). The architecture is controlled via three dynamically controlled beamsplitters. The first and last need only be on/off switches, whose sole purpose is to couple in the prepared pulse-train, keep it within the outer loop for the required duration, and then couple out of the outer loop, yielding the transformed pulse-train. The central beamsplitter must be able to implement arbitrary classically-controlled beamsplitter operations.

The workings of the scheme can be thought of as follows: the inner loop allows arbitrary beamsplitter operations between neighbouring time-bins; the outer loop does nothing interferometric, but rather enables the pulse-train to undergo as many applications of the inner loops as necessary. It then follows that this scheme is universal for linear optics, as a sufficient number of beamsplitter operations between neighbouring modes enables universal decompositions, using for example, the Reck *et al.* decomposition described earlier.

As a simple example of how such time-bin encoding maps to other encodings, in Fig. 5 we show the isomorphism between the polarising beamsplitter operation and a pairwise temporal beamsplitter operation. This implies a direct mapping for implementing cluster state preparation within the time-bin scheme.

The above description applies to passive linear optics, which is sufficient for protocols such as BOSON-SAMPLING, but insufficient for universal optical quantum computation, which requires the addition of ancillary states, and measurement with fast-feedforward. To address this, it was shown in (?) that by dynamically preparing ancillary pulse-trains (from the already-existing source), classically controlled by time-resolved measurements at the output, and changing the switching sequence, we can effectively couple in and out arbitrary subsets of the optical modes, enabling partial measurements to be implemented.

C. Photodetection

Broadly speaking, there are two main classes of photodetectors: non-photon-number-resolving (also referred to as bucket, or on/off) detectors, and photon-number-resolving (PNR) detectors. As the names suggest, non-PNR detectors only detect the presence or absence of photons in an incident beam, while PNR detectors are able to measure its number of photons. The outcomes of a PNR detector are described by the measurement projectors,

$$\hat{\Pi}_n = |n\rangle\langle n|, \ n = 0, 1, \dots \ , \tag{11}$$

while those of the non-photon-number-resolving detectors are given by

$$\hat{\Pi}_{\mathrm{off}} = \hat{\Pi}_0,$$
$$\hat{\Pi}_{\mathrm{on}} = \hat{I} - \hat{\Pi}_{\mathrm{on}} \ . \tag{12}$$

The dominant challenge facing the experimental implementation of both types of detectors is inefficiency due to loss, which results in higher photon-number being confused as having lower photon-number. In some protocols, such as type-II fusion, which relies on coincidence detection, inefficiency is not problematic. However, in most applications, including type-I fusion, this is highly problematic as photon-number confusion results in decoherence via projecting onto the wrong photon-number, unknown to the observer. Other common problems that
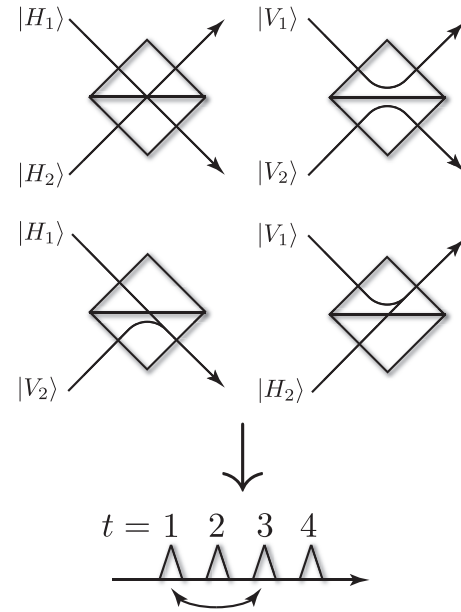

FIG. 5 Mapping between two polarisation-encoded qubits undergoing a polarising beamsplitter (PBS) operation, and its equivalent representation using 4 time-bins in a pulse-train. The PBS completely reflects (transmits) the vertical (horizontal) polarisations. The evolution of the four logical basis states, and their respective outputs, are shown explicitly. Writing out this PBS transformation in matrix form yields a permutation. Taking this permutation and relabelling the modes, we obtain the time-bin transformation shown underneath – a simple swap of two of the four time-bins.

plague these detectors are dark counts which add spurious counts from the background, and dead-time which causes the detector to lose counts during a period when it is inactive immediately after the detection of photons.

1. Non-photon-number-resolving detectors

The first type of non-PNR detectors are photomultiplier tubes (PMTs). A PMT comprises of a vacuum tube with a photocathode for light absorption. The photoelectric effect then releases electrons in the photocathode, and this current is multiplied by a cascade of secondary electron emissions from a series of electrodes. This amplified signal can be picked up to indicate the presence of photons.

In applications for quantum information processing, a well-established alternative to PMTs is the avalanche photodiode (APD). These are devices made up of semiconductor material, usually silicon, which is structured as a p-n junction and put into Geiger mode operation. When a photon is incident on the APD, electrons that are generated undergo an avalanche and the current that is generated can be measured. APDs are affordable, offer low dark count rates with reasonable efficiency, and can be made to operate in wavelengths in the visible to near-infrared range. A downside to using APD is their deadtime. This is a period of time following an avalanche during which the avalanche is stopped by a quenching circuit to reset the APD. No photons can be detected during the deadtime and contributes to photon loss in an APD.

The last type of non-PNR detectors we discuss is the superconducting nanowire single-photon detector (SNSPD) which have recently become commercially available. This detector uses a narrow superconducting wire that is carrying a current operating at just below the critical current density. Above this current density, the superconducting wire would undergo a phase change back to its normal resistance which happens when it absorbs an incident photon. The current in the wire would then by-pass it to go through the neighboring region which is still superconducting, and therefore at a lower resistance. This causes a voltage spike in the neighboring region which can be detected.

2. Photon-number-resolving detectors

Multiple technologies for realizing PNR detectors already exist and have been described by multiple reviews (Hadfield, 2009; Eisaman et al., 2011), so we shall only outline a few notable examples here. One of these is the superconducting transition edge sensor (TES) . In TES, a layer of superconducting material is operated at a temperature in its transition between superconducting and normal resistance. Any small change in temperature will thus cause a large change in resistance of this layer which

can be measured. This happens when photons are absorbed, and heats up the superconductor. Such detectors can be made so sensitive that the energy of single photons can be detected. Another advantage of the TES is its high efficiency which can be made very close to 100% (Rosenberg et al., 2005), and low dark count rates. However, they are quite slow, have low maximum counting rates, and are costly to operate due to their very low operating temperatures.

The visible light photon counter (VLPC) is another kind of PNR detector. The way VLPC works is in principle very similar to the APD. The top layer where the photon impinges is made of silicon, followed by another gain layer that is lightly doped with arsenic (As). When a photon is incident on this detector, it creates electrons which are then accelerated into the gain layer and ionize the As impurities, thereby exciting and scattering more electrons. An avalanche multiplication ensues just like in an APD. However, owing to the presence of the As gain later, the VLPC has a low multiplication noise which results in a single photon absorption event creating an electrical signal that is always of the same magnitude. Thus, the output electrical signal is just proportional to the number of detected photons.

Last, we discuss an approach to creating PNR detectors from non-PNR detectors by connecting a bunch of the latter in parallel to one another, and summing the signals at the output to give a combined signal that is proportional to that of just one. Such an approach has been demonstrated with SNSPD connected in parallel (Divochiy et al., 2008), and APDs connected in an array that can be either on the same semiconductor substrate, or as an interferometric architecture (Chen et al., 2017; Afek et al., 2009; Chrapkiewicz et al., 2014). A drawback of the parallel-SNSPDs is their low quantum efficiency, while the spatially multiplexed APDs suffer from spurious counts known as crosstalk that arises from avalanches triggered by electrons launched from neighboring APDs (Afek et al., 2009; Eraerds et al., 2007; Kalashnikov et al., 2012).

VII. APPLICATIONS FOR LINEAR OPTICS INTERFEROMETRY

A. Linear optics quantum computation (LOQC)

With the advancement in single-photon state preparation, detectors and quantum interferometers, quantum computation using linear optics has become feasible. For universal quantum computation using linear optics and single photon inputs, nonlinear couplings between the different optical modes are needed. Photons, being bosons, do not interact with one another like the way fermions do. Hence, some careful engineering has to be done in order to achieve this nonlinear coupling between modes. Some of the methods used to introduce this nonlinearity include measurements and feedforwarding (Knill et al.,

2001), and photon-atom interactions (Brod and Combes, 2016). These nonlinearities have been used to construct entangling gates required for (approximate) universality in quantum computation using the circuit model. They have also been used to construct entangled graph states, like the cluster states covered in Section VI.A.4, that are used in MBQC. Comprehensive reviews have been written previously to cover this topic (Pan et al., 2012; Kok et al., 2005), hence we will skip some basic information to focus on recent advances. There are multiple challenges to implementing a scalable, fully-optical quantum computer, and progress has been focused on overcoming these challenges. In this section, we will discuss a few of these challenges, and the advances that have been made to overcome them.

1. Challenges and Progress in LOQC

To date, the quantum computation still requires the use of non-deterministic operations, each of which succeeds with less than unity probability and has to be run many times before a single try succeeds. Moreover extra qubits are needed for error correction. These requirements put an overhead on the computational cost, in particular at the single photon production stage where a high rate of production of multiple photons is desired for this purpose. Second, feed-forwarding requires detectors with very fast response time. In feedforward control, one mode is measured and then some operation that depend on the measurement outcome are effected on other modes. The readout from the measurement has to happen before the light beam in the target modes passes. The last challenge is that of loss. Loss can happen anywhere in the linear optical network, but is especially problematic in coupling between different mediums, and upon absorption of a photon in a detector. Loss causes computations to fail. In the case that this error is detectable, the computation would have to be repeated. If not, the computation returns a wrong result.

Better single-photon sources that have been discussed in Section VI.A.1 are part of the solution to overcoming the above difficulties. Following the footsteps of implementing two-qubit gates using multiple degrees of freedom of single photons (Gasparoni et al., 2004; Zhao et al., 2005; Okamoto et al., 2005; Langford et al., 2005; Kiesel et al., 2005; Černoch et al., 2008; Gao et al., 2010; Zhou et al., 2011), improvement in our theoretical understanding have also led to more efficient designs of circuits (Zhou et al., 2011; Lanyon et al., 2009) that enabled the optical implementation of quantum teleportation of the state of a single photon (Wang et al., 2015). In this way, three-qubit (Lanyon et al., 2009; Mičuda et al., 2013; Patel et al., 2016) and four-qubit (Stárek et al., 2016) gates have also been implemented using LOQC.

If one wishes to avoid the use of non-deterministic quantum gates, the most promising alternative is to use cross-Kerr nonlinearities which have Hamiltonians for two modes labelled by a and b that is proportional to the form

$$a^\dagger(\omega)a(\omega)b^\dagger(\omega)b(\omega) \ . \tag{13}$$

Such Kerr nonlinearities are usually implemented on states of light via atom-photon interactions. Whether such cross-Kerr nonlinearities on single photon will help LOQC is a subject of debate. On one side, the arguments in the negative come down to fundamental noise limits in atom-photon interactions using phenomenological model of a cross-Kerr medium (Shapiro, 2006; Shapiro and Razavi, 2007; Gea-Banacloche, 2010). On the other hand, an example of a CPHASE gate using photons that counterpropagate through multiple atom-mediated cross-Kerr interaction sites has been constructed, and theoretically shown to work via a first principle treatment of the multimode light field and atomic medium (Brod and Combes, 2016). Regardless of who is right in this debate, increments in the strength of Kerr nonlinearities have been achieved in the last five years (Hoi et al., 2013; Venkataraman et al., 2013; Feizpour et al., 2015; Beck et al., 2016), and this avenue remains a tantalizing possibility for deterministic quantum gates.

The advent of integrated photonic circuits has greatly improved the feasibility of LOQC. A small chip on silica can contain what used to be spread over large optical tables in bulk optics. They also offer greater interferometric stability so that the requisite quantum interference to happen is less affected by changes in path lengths. These have been discussed at lengths in another review (Meany et al., 2015). Recent breakthroughs with programmable circuits have made a single chip reusable for different applications (Metcalf et al., 2014; Carolan et al., 2015). Previously, a different chip has to be manufactured every time a new interferometer setup is desired which is a waste of resources and requires a lead time for production.

Combining these chips with existing higher-efficiency sources and detectors will expand their capabilities. Loss can be mitigated by moving all components onto the same chip as the linear optical circuit (Sprengers et al., 2011; Silverstone et al., 2014). What remains is to have fast feedforward also on chip. This might pose the greatest challenge yet for universal LOQC. Only a handful of experiments have been able to implement adaptive feedforward for the purposes of LOQC (Prevedel et al., 2007; Ma et al., 2012; Miková et al., 2012; Zhao et al., 2014). The bottleneck is in the speed of modulation in the feedforward circuitry. The successful implementations of feedforward require the use of a delay loop to slow down the target photons so that the modulator has time to catch up.

Although there has been tremendous progress in pushing for an all-optical universal quantum computer with single photons, it seems likely that an efficient, and fault-tolerant universal quantum computer will require a hybrid system of photonics and something else. Nonetheless, linear optics alone is still a fascinating platform for

applications and foundational understanding of quantum mechanics.

B. Boson-sampling

Peter to do this.

C. Quantum metrology

An archetypal task for quantum metrology is the following: Given a Mach-Zedner interferometer, with an unknown phase shift of magnitude φ inserted in one of the two paths (see Fig. 6), can one deduce φ via a judicious use of quantum states and measurements with a higher sensitivity than that of a completely classical interferometer? It is well-known that one indeed can, and the standard deviation, $\Delta\varphi$, after N trials using quantum estimation is

$$\Delta\varphi = \frac{1}{N} \ , \qquad (14)$$

which gets a $\sqrt{N}$ improvement over classical phase estimation. As this sensitivity is also a fundamental limit arising from Heisenberg's uncertainty principle; we cannot measure definitively the phase, it is known as the Heisenberg limit. Most famously, a family of entangled states known as NOON states achieve this limit using N photons in a single trial. A NOON state is a superposition state in which N photons are either in the first or second path:

$$|\psi_n^{(\mathrm{NOON})}\rangle = \frac{1}{\sqrt{2}}(|N,0\rangle + |0,N\rangle) \ . \qquad (15)$$

Many reviews have been written for quantum metrology and Heisenberg-limited quantum phase estimation (Giovannetti et al., 2004; Dowling, 2008; Giovannetti et al., 2011) so we will not dwell on the history of this application. Instead, we will discuss a new paradigm for quantum metrology that has arisen from our understanding of Boson-sampling.

As discussed in Section VII.B, the resources needed for Boson-sampling is readily available, but executes a task that is believed to be hard classically. Surprisingly, an entanglement between a large number of spatial modes is possible with single photons in a passive linear optical device. This so-called number-path entanglement can be harnessed for quantum metrology without the use of entangled states like the NOON state (Motes et al., 2015). Here, the phase shift to be estimated, φ, manifests itself as a linear phase gradient across N modes (See Fig. 7). By straddling these modes among a quantum Fourier transform and its conjugate operation, it is possible to achieve

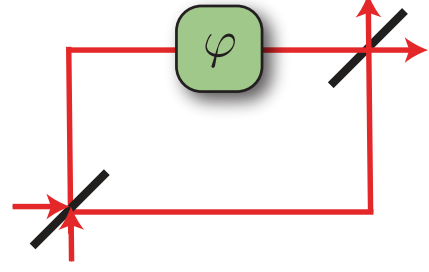$$\Delta\varphi = \mathcal{O}\left(\frac{1}{N^{3/2}}\right) \ , \qquad (16)$$

FIG. 6 A schematic diagram of the Mach-Zehnder interferometer comprising of two 50/50 beamsplitters with a phase shift φ in one of its two paths.

with just a string of N single photons, one photon per mode, for up to at least $N = 25$ modes.
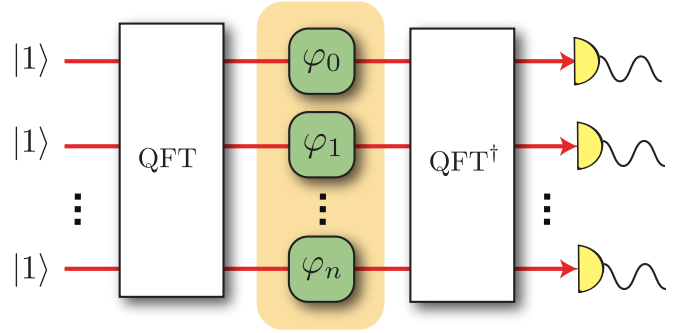

FIG. 7 Architecture of the quantum Fourier transform interferometer for metrology using single-photon states. QFT: Quantum Fourier transform circuit, and $\varphi_k = (k-1)\varphi$. Single photons are injected into the input modes on the left-hand-side, and a N-fold coincidence measurement is conducted at the output on the right-hand-side.

VIII. CONCLUSION

Linear optics interferometry has become a leading contender for the implementation of quantum information processing protocols. The preparation, manipulation and measurement of photonic quantum information has become mainstream and widely employed, with impressive experimental accuracies.

We have discussed the various ways in which quantum information can be represented photonically, how they can be manipulated and detected, and some of their leading applications.

Although there are countless physical architectures for the implementation of quantum information processing, and it is far from certain which will win 'the quantum race for supremacy, optics will always find a home as the only contender for applications involving quantum communication. For this reason, the future of linear optics

interferometry is a bright one, which will find inevitable applicability in the future quantum world.

Acknowledgments

References

M. Tillmann, S.-H. Tan, S. E. Stoeckl, B. C. Sanders, H. de Guise, R. Heilmann, S. Nolte, A. Szameit, and P. Walther, Phys. Rev. X **5**, 041015 (2015), URL http://link.aps.org/doi/10.1103/PhysRevX.5.041015.

N. Bozinovic, Y. Yue, Y. Ren, M. Tur, P. Kristensen, H. Huang, A. Willner, and S. Ramachandran, Science **340**, 1545 (2013).

A. Nicolas, L. Veissier, L. Giner, E. Giacobino, D. Maxein, and J. Laurat, Nat. Photonics **8**, 234 (2014).

P. C. Humphreys, B. J. Metcalf, J. B. Spring, M. Moore, X.-M. Jin, M. Barbieri, W. S. Kolthammer, and I. A. Walmsley, Phys. Rev. Lett. **111**, 150501 (2013), URL http://link.aps.org/doi/10.1103/PhysRevLett.111.150501.

J. M. Donohue, M. Agnew, J. Lavoie, and K. J. Resch, Phys. Rev. Lett. **111**, 153602 (2013), URL http://link.aps.org/doi/10.1103/PhysRevLett.111.153602.

M. Reck, A. Zeilinger, H. J. Bernstein, and P. Bertani, Phys. Rev. Lett. **73**, 58 (1994), URL http://link.aps.org/doi/10.1103/PhysRevLett.73.58.

I. Dhand and S. K. Goyal, Phys. Rev. A **92**, 043813 (2015), URL http://link.aps.org/doi/10.1103/PhysRevA.92.043813.

S.-H. Tan, Y. Y. Gao, H. de Guise, and B. C. Sanders, Phys. Rev. Lett. **110**, 113603 (2013), URL http://link.aps.org/doi/10.1103/PhysRevLett.110.113603.

H. de Guise, S.-H. Tan, I. P. Poulin, and B. C. Sanders, Phys. Rev. A **89**, 063819 (2014), URL http://link.aps.org/doi/10.1103/PhysRevA.89.063819.

H. de Guise, D. Spivak, J. Kulp, and I. Dhand, J. Phys. A:Math. Theor. **49**, 09LT01 (2016).

Y.-S. Ra, M. C. Tichy, H.-T. Lim, O. Kwon, F. Mintert, A. Buchleitner, and Y.-H. Kim, Proceedings of the National Academy of Sciences **110**, 1227 (2013), eprint http://www.pnas.org/content/110/4/1227.full.pdf, URL http://www.pnas.org/content/110/4/1227.abstract.

L.-A. Wu, P. Walther, and D. A. Lidar, Scientific Reports **3**, 1394 EP (2013), URL http://dx.doi.org/10.1038/srep01394.

J. Brendel, N. Gisin, W. Tittel, and H. Zbinden, Phys. Rev. Lett. **82**, 2594 (1999), URL https://link.aps.org/doi/10.1103/PhysRevLett.82.2594.

R. T. Thew, S. Tanzilli, W. Tittel, H. Zbinden, and N. Gisin, Phys. Rev. A **66**, 062304 (2002), URL https://link.aps.org/doi/10.1103/PhysRevA.66.062304.

I. Marcikic, H. de Riedmatten, W. Tittel, H. Zbinden, M. Legré, and N. Gisin, Phys. Rev. Lett. **93**, 180502 (2004), URL https://link.aps.org/doi/10.1103/PhysRevLett.93.180502.

E. Knill, R. Laflamme, and G. Milburn, Nature (London) **409**, 46 (2001).

K. R. Motes, A. Gilchrist, J. P. Dowling, and P. P. Rohde, Phys. Rev. Lett. **113**, 120501 (2014), URL https://link.aps.org/doi/10.1103/PhysRevLett.113.120501.

B.-G. Englert, C. Kurtsiefer, and H. Weinfurter, Phys. Rev. A **63**, 032303 (2001), URL https://link.aps.org/doi/10.1103/PhysRevA.63.032303.

A. Bouland and S. Aaronson, Phys. Rev. A **89**, 062316 (2014), URL https://link.aps.org/doi/10.1103/PhysRevA.89.062316.

M. W. Mitchell, C. W. Ellenor, S. Schneider, and A. M. Steinberg, Phys. Rev. Lett. **91**, 120402 (2003).

J. L. O'Brien, G. J. Pryde, A. Gilchrist, D. F. V. James, N. K. Langford, T. C. Ralph, and A. G. White, Phys. Rev. Lett. **93**, 080502 (2004), URL https://link.aps.org/doi/10.1103/PhysRevLett.93.080502.

M. Lobino, D. Korystov, C. Kupchak, E. Figueroa, B. C. Sanders, and A. I. Lvovsky, Science **322**, 563 (2008), ISSN 0036-8075, eprint http://science.sciencemag.org/content/322/5901/563.full.pdf, URL http://science.sciencemag.org/content/322/5901/563.

S. Rahimi-Keshari, A. Scherer, A. Mann, A. T. Rezakhani, A. I. Lvovsky, and B. C. Sanders, New Journal of Physics **13**, 013006 (2011), URL http://stacks.iop.org/1367-2630/13/i=1/a=013006.

N. C. Harris, D. Bunandar, M. Pant, G. R. Steinbrecher, J. Mower, M. Prabhu, T. Baehr-Jones, M. Hochberg, and D. Englund, Nanophotonics **5** (2016), URL https://www.degruyter.com/view/j/nanoph.ahead-of-print/nanoph-2015-0146/nanoph-2015-0146.xml.

A. Laing and J. O'Brien, arXiv: 1208.2868v1 (2012).

S. Rahimi-Keshari, M. A. Broome, R. Fickler, A. Fedrizzi, T. C. Ralph, and A. G. White, Opt. Express **21**, 13450 (2013), URL http://www.opticsexpress.org/abstract.cfm?URI=oe-21-11-13450.

I. Dhand, A. Khalid, H. Lu, and B. C. Sanders, Journal of Optics **18**, 035204 (2016), URL http://stacks.iop.org/2040-8986/18/i=3/a=035204.

N. Spagnolo, E. Maiorino, C. Vitelli, M. Bentivegna, A. Crespi, R. Ramponi, P. Mataloni, R. Osellame, and F. Sciarrino (2016), eprint arXiv:1610.03291v1.

M. Tillmann, C. Schmidt, and P. Walther, Journal of Optics **18**, 114002 (2016), URL http://stacks.iop.org/2040-8986/18/i=11/a=114002.

R. Heilmann, M. Grfe, S. Nolte, and A. Szameit, Science Bulletin **60**, 96 (2015), ISSN 2095-9273, URL http://www.sciencedirect.com/science/article/pii/S2095927316305400.

X.-L. Wang, L.-K. Chen, W. Li, H.-L. Huang, C. Liu, C. Chen, Y.-H. Luo, Z.-E. Su, D. Wu, Z.-D. Li, et al., Phys. Rev. Lett. **117**, 210502 (2016a), URL https://link.aps.org/doi/10.1103/PhysRevLett.117.210502.

L.-K. Chen, Z.-D. Li, X.-C. Yao, M. Huang, W. Li, H. Lu, X. Yuan, Y.-B. Zhang, X. Jiang, C.-Z. Peng, et al., Optica **4**, 77 (2017), URL http://www.osapublishing.org/optica/abstract.cfm?URI=optica-4-1-77.

H. Wang, Y. He, Y.-H. Li, Z.-E. Su, B. Li, H.-L. Huang, X. Ding, M.-C. Chen, C. Liu, J. Qin, et al. (2016b), eprint quant-ph:1612.06956.

A. Muller, E. B. Flagg, P. Bianucci, X. Y. Wang, D. G. Deppe,

W. Ma, J. Zhang, G. J. Salamo, M. Xiao, and C. K. Shih, Phys. Rev. Lett. **99**, 187402 (2007), URL https://link.aps.org/doi/10.1103/PhysRevLett.99.187402.

A. Nick Vamivakas, Y. Zhao, C.-Y. Lu, and M. Atature, Nat Phys **5**, 198 (2009), URL http://dx.doi.org/10.1038/nphys1182.

E. B. Flagg, A. Muller, J. W. Robertson, S. Founta, D. G. Deppe, M. Xiao, W. Ma, G. J. Salamo, and C. K. Shih, Nat Phys **5**, 203 (2009), URL http://dx.doi.org/10.1038/nphys1184.

S. Ates, S. M. Ulrich, S. Reitzenstein, A. Löffler, A. Forchel, and P. Michler, Phys. Rev. Lett. **103**, 167402 (2009), URL https://link.aps.org/doi/10.1103/PhysRevLett.103.167402.

D. Englund, A. Majumdar, A. Faraon, M. Toishi, N. Stoltz, P. Petroff, and J. Vučković, Phys. Rev. Lett. **104**, 073904 (2010), URL https://link.aps.org/doi/10.1103/PhysRevLett.104.073904.

Y.-M. He, Y. He, Y.-J. Wei, D. Wu, M. Atature, C. Schneider, S. Hofling, M. Kamp, C.-Y. Lu, and J.-W. Pan, Nat Nano **8**, 213 (2013a), URL http://dx.doi.org/10.1038/nnano.2012.262.

H. Jayakumar, A. Predojević, T. Huber, T. Kauten, G. S. Solomon, and G. Weihs, Phys. Rev. Lett. **110**, 135505 (2013), URL https://link.aps.org/doi/10.1103/PhysRevLett.110.135505.

Y.-J. Wei, Y.-M. He, M.-C. Chen, Y.-N. Hu, Y. He, D. Wu, C. Schneider, M. Kamp, S. Hfling, C.-Y. Lu, et al., Nano Letters **14**, 6515 (2014), pMID: 25357153, eprint http://dx.doi.org/10.1021/nl503081n, URL http://dx.doi.org/10.1021/nl503081n.

M. Muller, S. Bounouar, K. D. Jons, M. Glassl, and M. P., Nat Photon **8**, 224 (2014), URL http://dx.doi.org/10.1038/nphoton.2013.377.

S. Unsleber, C. Schneider, S. Maier, Y.-M. He, S. Gerhardt, C.-Y. Lu, J.-W. Pan, M. Kamp, and S. Höfling, Opt. Express **23**, 32977 (2015), URL http://www.opticsexpress.org/abstract.cfm?URI=oe-23-26-32977.

Y. He, Y.-M. He, Y.-J. Wei, X. Jiang, M.-C. Chen, F.-L. Xiong, Y. Zhao, C. Schneider, M. Kamp, S. Höfling, et al., Phys. Rev. Lett. **111**, 237403 (2013b), URL https://link.aps.org/doi/10.1103/PhysRevLett.111.237403.

T. M. Sweeney, S. G. Carter, A. S. Bracker, M. Kim, C. S. Kim, L. Yang, P. M. Vora, P. G. Brereton, E. R. Cleveland, and D. Gammon, Nat Photon **8**, 442 (2014), URL http://dx.doi.org/10.1038/nphoton.2014.84.

X. Ding, Y. He, Z.-C. Duan, N. Gregersen, M.-C. Chen, S. Unsleber, S. Maier, C. Schneider, M. Kamp, S. Höfling, et al., Phys. Rev. Lett. **116**, 020401 (2016), URL https://link.aps.org/doi/10.1103/PhysRevLett.116.020401.

H. Wang, Z.-C. Duan, Y.-H. Li, S. Chen, J.-P. Li, Y.-M. He, M.-C. Chen, Y. He, X. Ding, C.-Z. Peng, et al., Phys. Rev. Lett. **116**, 213601 (2016c), URL https://link.aps.org/doi/10.1103/PhysRevLett.116.213601.

Y.-H. Kim, S. P. Kulik, and Y. Shih, Phys. Rev. A **63**, 060301 (2001), URL https://link.aps.org/doi/10.1103/PhysRevA.63.060301.

Y.-H. Kim, S. P. Kulik, M. V. Chekhova, W. P. Grice, and Y. Shih, Phys. Rev. A **67**, 010301 (2003), URL https://link.aps.org/doi/10.1103/PhysRevA.67.010301.

G. Brida, M. Chekhova, M. Genovese, and L. Krivitsky, Phys. Rev. A **76**, 053807 (2007), URL https://link.aps.org/doi/10.1103/PhysRevA.76.053807.

B. Dayan, Y. Bromberg, I. Afek, and Y. Silberberg, Phys.

Rev. A **75**, 043804 (2007), URL https://link.aps.org/doi/10.1103/PhysRevA.75.043804.

T. B. Pittman, M. M. Donegan, M. J. Fitch, B. C. Jacobs, J. D. Franson, P. Kok, H. Lee, and J. P. Dowling, IEEE Journal of Selected Topics in Quantum Electronics **9**, 1478 (2003), ISSN 1077-260X.

C. Śliwa and K. Banaszek, Phys. Rev. A **67**, 030101 (2003), URL https://link.aps.org/doi/10.1103/PhysRevA.67.030101.

P. Walther, M. Aspelmeyer, and A. Zeilinger, Phys. Rev. A **75**, 012313 (2007), URL https://link.aps.org/doi/10.1103/PhysRevA.75.012313.

C. Wagenknecht, C.-M. Li, A. Reingruber, X.-H. Bao, A. Goebel, Y.-A. Chen, Q. Zhang, K. Chen, and J.-W. Pan, Nat Photon **4**, 549 (2010), URL http://dx.doi.org/10.1038/nphoton.2010.123.

S. Barz, G. Cronenberg, A. Zeilinger, and P. Walther, Nat Photon **4**, 553 (2010), URL http://dx.doi.org/10.1038/nphoton.2010.156.

D. M. Greenberger, M. A. Horne, and A. Z. (edited by M. Kafatos), *Going beyond Bell's theorem* (Kluwer Academic, Dordrecht, The Netherlands, 1989), p. 73.

J.-W. Pan, D. Bouwmeester, M. Daniell, H. Weinfurter, and A. Zeilinger, Nature **403**, 515 (2000), URL http://dx.doi.org/10.1038/35000514.

C. Zhang, Y.-F. Huang, Z. Wang, B.-H. Liu, C.-F. Li, and G.-C. Guo, Phys. Rev. Lett. **115**, 260402 (2015), URL https://link.aps.org/doi/10.1103/PhysRevLett.115.260402.

J.-W. Pan, Z.-B. Chen, C.-Y. Lu, H. Weinfurter, A. Zeilinger, and M. Żukowski, Rev. Mod. Phys. **84**, 777 (2012), URL https://link.aps.org/doi/10.1103/RevModPhys.84.777.

H. J. Briegel and R. Raussendorf, Phys. Rev. Lett. **85**, 910 (2001).

R. Raussendorf, D. E. Browne, and H. J. Briegel, Phys. Rev. A **68**, 022312 (2003).

R. H. Hadfield, Nat Photon **3**, 696 (2009), URL http://dx.doi.org/10.1038/nphoton.2009.230.

M. Eisaman, J. Fan, A. Migdall, and S. Polyakov, Review of Scientific Instruments **82** (2011), URL http://aip.scitation.org/doi/full/10.1063/1.3610677.

D. Rosenberg, A. E. Lita, A. J. Miller, and S. W. Nam, Phys. Rev. A **71**, 061803(R) (2005).

A. Divochiy, F. Marsili, D. Bitauld, A. Gaggero, R. Leoni, F. Mattioli, A. Korneev, V. Seleznev, N. Kaurova, O. Minaeva, et al., Nat Photon **2**, 302 (2008), URL http://dx.doi.org/10.1038/nphoton.2008.51.

I. Afek, A. Natan, O. Ambar, and Y. Silberberg, Phys. Rev. A **79**, 043830 (2009), URL https://link.aps.org/doi/10.1103/PhysRevA.79.043830.

R. Chrapkiewicz, W. Wasilewski, and K. Banaszek, Opt. Lett. **39**, 5090 (2014), URL http://ol.osa.org/abstract.cfm?URI=ol-39-17-5090.

P. Eraerds, M. Legré, A. Rochas, H. Zbinden, and N. Gisin, Opt. Express **15**, 14539 (2007), URL http://www.opticsexpress.org/abstract.cfm?URI=oe-15-22-14539.

D. A. Kalashnikov, S.-H. Tan, T. S. Iskhakov, M. V. Chekhova, and L. A. Krivitsky, Opt. Lett. **37**, 2829 (2012), URL http://ol.osa.org/abstract.cfm?URI=ol-37-14-2829.

D. J. Brod and J. Combes, Phys. Rev. Lett. **117**, 080502 (2016), URL https://link.aps.org/doi/10.1103/PhysRevLett.117.080502.

P. Kok, W. J. Munro, K. Nemoto, T. C. Ralph, J. P. Dowling, and G. J. Milburn, Rev. Mod. Phys. **79**, 135 (2005).

S. Gasparoni, J.-W. Pan, P. Walther, T. Rudolph, and A. Zeilinger, Phys. Rev. Lett. **93**, 020504 (2004).

Z. Zhao, A.-N. Zhang, Y.-A. Chen, H. Zhang, J.-F. Du, T. Yang, and J.-W. Pan, Phys. Rev. Lett. **94**, 030501 (2005).

R. Okamoto, H. F. Hofmann, S. Takeuchi, and K. Sasaki, Phys. Rev. Lett. **95**, 210506 (2005), URL https://link.aps.org/doi/10.1103/PhysRevLett.95.210506.

N. K. Langford, T. J. Weinhold, R. Prevedel, K. J. Resch, A. Gilchrist, J. L. O'Brien, G. J. Pryde, and A. G. White, Phys. Rev. Lett. **95**, 210504 (2005), URL https://link.aps.org/doi/10.1103/PhysRevLett.95.210504.

N. Kiesel, C. Schmid, U. Weber, R. Ursin, and H. Weinfurter, Phys. Rev. Lett. **95**, 210505 (2005), URL https://link.aps.org/doi/10.1103/PhysRevLett.95.210505.

A. Černoch, J. Soubusta, L. Bartůšková, M. Dušek, and J. Fiurášek, Phys. Rev. Lett. **100**, 180501 (2008), URL https://link.aps.org/doi/10.1103/PhysRevLett.100.180501.

W.-B. Gao, A. M. Goebel, C.-Y. Lu, H.-N. Dai, C. Wagenknecht, Q. Zhang, B. Zhao, C.-Z. Peng, Z.-B. Chen, Y.-A. Chen, et al., Proceedings of the National Academy of Sciences **107**, 20869 (2010), eprint http://www.pnas.org/content/107/49/20869.full.pdf, URL http://www.pnas.org/content/107/49/20869.abstract.

X.-Q. Zhou, T. C. Ralph, P. Kalasuwan, M. Zhang, A. Peruzzo, B. P. Lanyon, and J. L. O'Brien, Nature Communications **2**, 413 EP (2011), URL http://dx.doi.org/10.1038/ncomms1392.

B. P. Lanyon, M. Barbieri, M. P. Almeida, T. Jennewein, T. C. Ralph, K. J. Resch, G. J. Pryde, J. L. O/'Brien, A. Gilchrist, and A. G. White, Nat Phys **5**, 134 (2009), URL http://dx.doi.org/10.1038/nphys1150.

X.-L. Wang, X.-D. Cai, Z.-E. Su, M.-C. Chen, D. Wu, L. Li, N.-L. Liu, C.-Y. Lu, and J.-W. Pan, Nature **518**, 516 (2015), URL http://dx.doi.org/10.1038/nature14246.

M. Mičuda, M. Sedlák, I. Straka, M. Miková, M. Dušek, M. Ježek, and J. Fiurášek, Phys. Rev. Lett. **111**, 160407 (2013), URL https://link.aps.org/doi/10.1103/PhysRevLett.111.160407.

R. B. Patel, J. Ho, F. Ferreyrol, T. C. Ralph, and G. J. Pryde, Science Advances **2** (2016), eprint http://advances.sciencemag.org/content/2/3/e1501531.full.pdf, URL http://advances.sciencemag.org/content/2/3/e1501531.

R. Stárek, M. Mičuda, M. Miková, I. Straka, M. Dušek, M. Ježek, and J. Fiurášek, Scientific Reports **6**, 33475 EP (2016), URL http://dx.doi.org/10.1038/srep33475.

J. H. Shapiro, Phys. Rev. A **73**, 062305 (2006), URL https://link.aps.org/doi/10.1103/PhysRevA.73.062305.

J. H. Shapiro and M. Razavi, New J. Phys. **9**, 16 (2007).

J. Gea-Banacloche, Phys. Rev. A **81**, 043823 (2010), URL https://link.aps.org/doi/10.1103/PhysRevA.81.043823.

I.-C. Hoi, A. F. Kockum, T. Palomaki, T. M. Stace, B. Fan, L. Tornberg, S. R. Sathyamoorthy, G. Johansson, P. Delsing, and C. M. Wilson, Phys. Rev. Lett. **111**, 053601 (2013), URL https://link.aps.org/doi/10.1103/PhysRevLett.111.053601.

V. Venkataraman, K. Saha, and A. L. Gaeta, Nat Photon **7**, 138 (2013), URL http://dx.doi.org/10.1038/nphoton.2012.283.

A. Feizpour, M. Hallaji, G. Dmochowski, and A. M. Steinberg, Nat Phys **11**, 905 (2015), URL http://dx.doi.org/10.1038/nphys3433.

K. M. Beck, M. Hosseini, Y. Duan, and V. Vuleti?, Proceedings of the National Academy of Sciences **113**, 9740 (2016), eprint http://www.pnas.org/content/113/35/9740.full.pdf, URL http://www.pnas.org/content/113/35/9740.abstract.

T. Meany, M. Grä fe, R. Heilmann, A. Perez-Leija, S. Gross, M. J. Steel, M. J. Withford, and A. Szameit, Laser & Photonics Reviews **9**, 363 (2015), ISSN 1863-8899, URL http://dx.doi.org/10.1002/lpor.201500061.

B. J. Metcalf, J. B. Spring, P. C. Humphreys, N. Thomas-Peter, M. Barbieri, W. S. Kolthammer, X.-M. Jin, N. K. Langford, D. Kundys, J. C. Gates, et al., Nat Photon **8**, 770 (2014), URL http://dx.doi.org/10.1038/nphoton.2014.217.

J. Carolan, C. Harrold, C. Sparrow, E. Martín-López, N. J. Russell, J. W. Silverstone, P. J. Shadbolt, N. Matsuda, M. Oguma, M. Itoh, et al., Science (2015), ISSN 0036-8075, eprint http://science.sciencemag.org/content/early/2015/07/08/science.aab36, URL http://science.sciencemag.org/content/early/2015/07/08/science.aab3642.

J. P. Sprengers, A. Gaggero, D. Sahin, S. Jahanmirinejad, G. Frucci, F. Mattioli, R. Leoni, J. Beetz, M. Lermer, M. Kamp, et al., Applied Physics Letters **99**, 181110 (2011), eprint http://dx.doi.org/10.1063/1.3657518, URL http://dx.doi.org/10.1063/1.3657518.

J. W. Silverstone, D. Bonneau, K. Ohira, N. Suzuki, H. Yoshida, N. Iizuka, M. Ezaki, C. M. Natarajan, M. G. Tanner, R. H. Hadfield, et al., Nat Photon **8**, 104 (2014), URL http://dx.doi.org/10.1038/nphoton.2013.339.

R. Prevedel, P. Walther, F. Tiefenbacher, P. Bohi, R. Kaltenbaek, T. Jennewein, and A. Zeilinger, Nature **445**, 65 (2007), URL http://dx.doi.org/10.1038/nature05346.

X.-S. Ma, T. Herbst, T. Scheidl, D. Wang, S. Kropatschek, W. Naylor, B. Wittmann, A. Mech, J. Kofler, E. Anisimova, et al., Nature **489**, 269 (2012), URL http://dx.doi.org/10.1038/nature11472.

M. Miková, H. Fikerová, I. Straka, M. Mičuda, J. Fiurášek, M. Ježek, and M. Dušek, Phys. Rev. A **85**, 012305 (2012), URL https://link.aps.org/doi/10.1103/PhysRevA.85.012305.

T.-M. Zhao, H. Zhang, J. Yang, Z.-R. Sang, X. Jiang, X.-H. Bao, and J.-W. Pan, Phys. Rev. Lett. **112**, 103602 (2014), URL https://link.aps.org/doi/10.1103/PhysRevLett.112.103602.

V. Giovannetti, S. Lloyd, and L. Maccone, Science **306**, 1330 (2004), ISSN 0036-8075, eprint http://science.sciencemag.org/content/306/5700/1330.full.pdf, URL http://science.sciencemag.org/content/306/5700/1330.

J. P. Dowling, Contemporary Physics **49**, 125 (2008), eprint http://dx.doi.org/10.1080/00107510802091298, URL http://dx.doi.org/10.1080/00107510802091298.

V. Giovannetti, S. Lloyd, and L. Maccone, Nat Photon **5**, 222 (2011), URL http://dx.doi.org/10.1038/nphoton.2011.35.

K. R. Motes, J. P. Olson, E. J. Rabeaux, J. P. Dowling, S. J. Olson, and P. P. Rohde, Phys. Rev. Lett. **114**, 170802 (2015), URL https://link.aps.org/doi/10.1103/PhysRevLett.114.170802.